Investigation of thermo-structural behaviors of different ventilation applications on brake discs [†]

Mesut Duzgun[*]

Automotive Engineering Department, Faculty of Technology, Gazi University, 06500, Ankara, Turkey

---

Abstract

One of the most common problems related to brake discs is overheating, which negatively affects braking performance especially under the continuous braking conditions of vehicles. Ventilation applications on brake discs can significantly improve the brake system performance by reducing the heating of the discs. In this study, the thermal behaviors of ventilated brake discs using three different configurations were investigated at continuous brake conditions in terms of heat generation and thermal stresses with finite element analysis. The results were compared with a solid disc. Heat generation on solid brake discs reduced to a maximum of 24% with ventilation applications. The experimental study indicated finite element temperature analysis results in the range between 1.13% and 10.87%. However, thermal stress formations were higher with ventilated brake discs in comparison to those with solid discs.

Keywords: Brake discs; Heat generation; Thermo-structural behaviors; Ventilation applications

---

1. Introduction

Ventilated brake discs or rotors are known as high-performance brakes, and are produced by making hollows or slots (or both) of different shapes on disc surfaces and side edges. Ventilated brake discs were originally tested on racing cars in the 1960s, and they have been employed widely in the automotive and railway industry using different designs [1, 2]. During braking, kinetic energy is converted to heat. Around 90% of this energy is absorbed by the brake disc and then transferred to ambient air. Solid brake discs dissipate heat slowly. Therefore, ventilated brake discs are used to improve cooling by facilitating air circulation [3, 4]. They generally exhibit convective heat transfer coefficients approximately twice as large as those associated with solid discs [5].

There are numerous studies related to ventilation applications on brake discs. Zuber and Heidenreich [6] manufactured three different ventilated brake disc constructions from carbon fiber-reinforced ceramic matrix composites (CMC) and compared their strengths. Antanaitis and Rifici [7] proved that the 90-hole cross-drilled pattern improved heat rejection capability of the disc between 8.8% and 20.1% depending on the vehicle speed. Aleksendric et al. [8] showed the ability of a ventilated brake disc rotor in dissipating thermal flow by finite element analysis (FEA). Venkitachalam and Maharudrappa [9] conducted flow and heat transfer analysis of six different types of disc configurations by computational fluid dynamics (CFD) and recommended ventilated brake discs for high-speed vehicles. Park et al. [10] designed a helical surface inside vanes for a ventilated brake disc. They optimized Reynolds (Re), Prandtl (Pr), and Nusselt (Nu) numbers for their design and obtained improvements to a maximum of 44% in heat transfer. Improvement in brake fade resistance and higher braking performance in wet conditions are some other useful aspects of ventilated brake discs. However, they also have some disadvantages. Cracking, is one of them and this a phenomenon that has been correlated to stresses during braking [11]. Kim et al. [12] showed the maximum von-Mises stress generation of actual fatigue cracks located on ventilated brake discs of railway vehicles by thermal stress analysis. Similarly, Bagnoli et al. [13] performed FEA to determine the temperature profile and to estimate the von-Mises stress distribution that arises during braking for fire-fighting vehicles. Hwang and Wu [14] investigated temperature and thermal stress in a ventilated brake disc based on a thermo-mechanical coupling model. Decreasing the brake temperatures and/or re-designing the hub-rotor unit were some considerable conclusions of Mackin et al. [15] to eliminate cracking in brake rotors. Heat generation also affects thermo-mechanical instability of brake discs [16].

Previous literature focused on heat and stress formations on ventilated discs. In this study, FEA was used to investigate the

---

Table 1. Mechanical and thermal properties of brake discs and pads.

Mechanical and thermal properties	Disc	Pad
Young's modulus (N/mm^2)	110000	1500
Poisson's ratio	0.28	0.25
Density (kg/m^3)	7200	2595
Thermal expansion (1/°C)	1.1e–005	6.6e–005
Tensile ultimate strength (N/mm^2)	240	-
Compressive ultimate strength (N/mm^2)	820	-
Coefficient of friction	0.35	0.35
Thermal conductivity (W/m°C)	52	1.212
Specific heat (J/kg°C)	447	1465

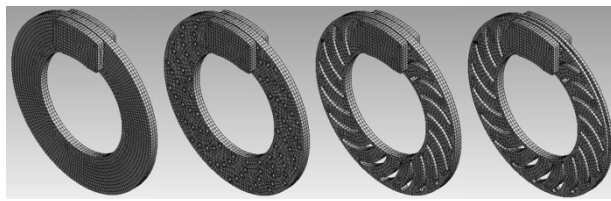(a) SL disc   (b) CD disc   (c) CS disc   (d) CS-SG disc

Fig. 1. Finite element mesh models.

thermal behavior of three different ventilated brake designs: cross-drilled (CD), cross-slotted (CS), and cross-slotted with side groove (CS-SG) discs. The results were then compared to a solid (SL) disc. An experimental study was also performed to verify the FEA results.

2. Thermo-structural FEA

For FEA, three-dimensional (3D) constructions of brake discs, brake pads, and their assembly designs were modeled with 1/1 scale in a software program, and then imported into another software program for the interactive thermo-structural analyses. Brake discs and brake pads were modeled by Quadratic Hexahedron mesh types.

Quadratic Hexahedron mesh generations are known for their accuracy and computational efficiency [17]. A frictional contact pair having the element type of Quadratic Quadrilateral Contact was defined between disc-pad interfaces. Fig. 1 shows the mesh models of the disc-pad systems.

Grey cast iron, a commonly used disc material, was used for the brake discs. The mechanical and thermal properties of the brake discs and pads are given in Table 1.

Ventilated brake discs were designed according to the propeller-shaped methodology for the hole and slot locations. For the CD disc, five holes with 5.2 mm diameter were arranged at equal intervals on an arc with a length of 60.54 mm. These holes were duplicated in groups of 20 on the disc surface. Thus, a total of 100 holes were drilled on the disc surface of

the CD disc. For the CS disc, 20 channels (6.9 mm wide and 67.3 mm long) were placed on a solid disc surface. Finally, the CS-SG disc was designed by making a groove (4 mm wide and 15 mm deep) on another CS disc edge. Hence, a path opening to the outer disc side edge was obtained to provide better air circulation.

2.1 Thermal analysis

For the thermal analysis, the ambient temperature was assumed at 22°C and the disc surface temperature was 100°C prior to braking, which was related with cold braking performance [8]. The current study assumed that heat dissipation from the brake disc to the atmosphere occurs via convection, also known as Newton's law of cooling. Convection is governed by Eq. (1), where Q is the rate of heat transfer (W), h is the convection heat transfer coefficient, A is the surface area of the rotor (m^2), T_s is the surface temperature of the brake rotor (°C), and T_∞ is the ambient air temperature (°C). The convection heat transfer coefficient is applied to the body of the brake discs as the boundary condition. Thus, to increase heat transfer from the brake discs and to reduce the disc surface temperature on the total surface area of the brake discs, the heat transfer coefficients were gradually increased by employing ventilation applications.

$$Q = h.A.(T_S - T_\infty) \tag{1}$$

The heat transfer coefficient associated with laminar flow for solid or non-ventilated brake discs was derived by Eq. (2) (for $Re < 2.4 \times 10^5$) [5], where D is the outer diameter of the discs (mm), Re is the Reynolds number, and k_a is the thermal conductivity of air ($W/m°C$).

$$h_R = 0.70(k_a / D)\mathrm{Re}^{0.55} \tag{2}$$

Meanwhile, the heat transfer coefficient associated with laminar flow for ventilated brake discs was approximated by Eq. (3) (for laminar flow condition, $Re < 10^4$) [5], where Pr is the Prandtl number, d_h is the hydraulic diameter (mm), and l is the length of the cooling vane (mm). The hydraulic diameter (d_h) is defined as the ratio of four times the cross-sectional flow area (wetted area) of the hole and slots in ventilated brake discs divided by their wetted perimeters as illustrated in Fig. 2.

$$h_R = 1.86(RePr)^{1/3}(d_h / l)^{0.33}(k_a / d_h) \tag{3}$$

In this condition, Re number is associated with the velocity of the air flow present in the hole and slot-shaped vanes as determined by Eq. (4), where ρ_a is the density of air (kg/mm^3), m_a is the mass flow rate of air (m^3/sec), and $V_{average}$ is the average velocity (m/sec).
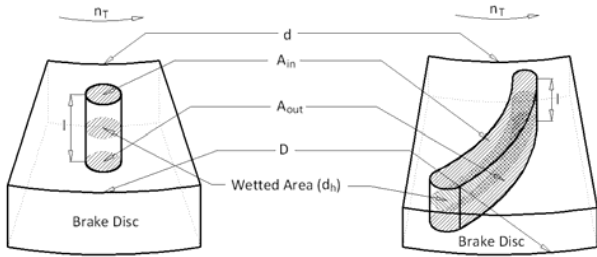
Fig. 2. Wetted areas (hydraulic diameter, d_h), length of hole and slot-shaped cooling vanes, and inlet and outlet areas for air flow of ventilated brake discs used in this study.
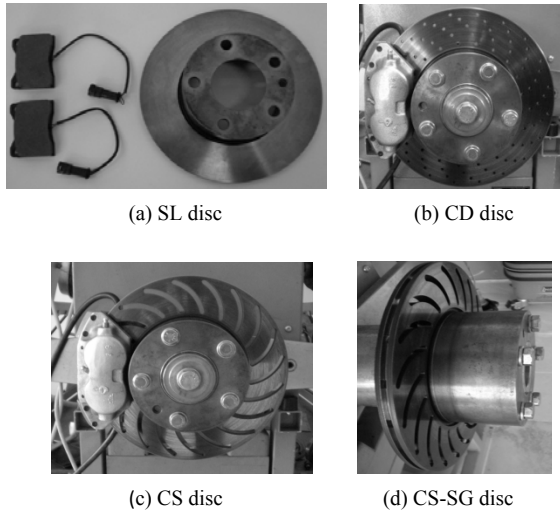

(a) SL disc (b) CD disc

(c) CS disc (d) CS-SG disc

Fig. 3. Brake caliper and brake discs.

$$\text{Re} = (\rho_a d_h / m_a) V_{average} \qquad (4)$$

The average speed can be calculated by Eq. (5), where n_T is the revolutions per minute (*1/min, rpm*), D is the outer diameter of the disc (*mm*), d is the inner diameter of the disc (*mm*), A_{out} is the outlet area of the hole or slot-shaped vanes (*mm²*), and A_{in} is the inlet area of the hole or slot-shaped vanes (*mm²*).

$$V_{average} = [0.0158 n_T \sqrt{D^2 - d^2} ([A_{out} + A_{in}]/A_{out}])]$$
$$(5)$$

Moreover, the air flow rate m_a is determined by Eq. (6):

$$m_a = 0.00147 n_T \sqrt{(D^2 - d^2) A_{in}} \,(m^3/\text{sec}) . \qquad (6)$$

2.1.1 Experimental study

The experimental study was performed to examine temperature changes on disc surfaces. For this purpose, the ventilated brake discs were manufactured from the Alfred Teves (ATE) solid discs to obtain their design characteristics. The CD and CS discs were manufactured on a three-axis CNC
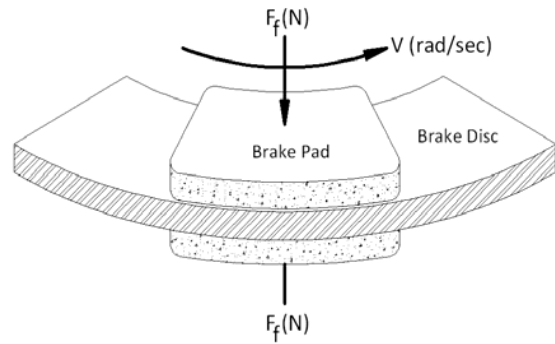

Fig. 4. Structural model for the brake discs.

Vertical Machining Centre. The side groove for the CS-SG disc was made on a CNC Turning Centre. The disc temperature outputs were measured on a brake test system. This system consists of a caliper mechanism as seen in Fig. 3, a piezo crystal force measurement system for pedal and brake force variations, a driving engine, a gear box, and indicators for brake/pedal forces and temperature.

For the temperature measurement, a thermocouple mounted on the caliper system was used. The power of the motor was 4 kW. The rotation of the discs was on a clockwise direction. ATE 501 FF brake pads were used in the experiments. Experiments were conducted under continuous braking conditions at a constant pedal force of 250 N, and eight periodic measurements of braking temperature were executed at 30, 60, 90, 120, 150, 180, 210 and 240 s.

2.2 Structural analysis

Disc temperatures obtained by thermal analyses were imported into the structural analytical models as boundary conditions. In the structural analyses, 9689 N equivalent to 250 N pedal force was applied on each top surface of the brake pads at a revolution speed of 60 km/h (or angular velocity of 52.56 rad/s) as seen in Fig. 4. The rate of the disc was assumed to be constant and the time required for a complete stop was 240 s.

The value of the pedal force was obtained by Eq. (7) [18], where F_f is the force on each front cylinder piston, F is the force on the foot pedal, A_f is the cross-sectional area of the front pistons, A_m is the cross-sectional area of the master cylinder, p_n is the number of pistons, *2.3* is the pedal leverage ratio, and *2.75* is the effect of servo unit.

$$F_f = \frac{F.A_f.p_n.2,3.2,75}{A_m} \qquad (7)$$

This computation was done according to the test equipment used in the experimental study. The pedal force leverage ratio and the servo unit effect are the values of the test equipment. Analyses were simulated according to the equivalent (von-Mises) stress distributions.

Table 2. Experimental and FEA results for disc temperatures.

Time (sec.)	SL disc		CD disc	
	Exp. temp. (°C)	FEA temp. (°C)	Exp. temp. (°C)	FEA temp. (°C)
30	124	137.49	156	169.99
60	189	174.97	219	200.02
90	238	212.44	254	230.06
120	276	249.92	291	260.09
150	318	287.40	321	290.13
180	358	324.87	345	320.16
210	378	362.35	355	350.20
240	395	399.82	371	380.23
Time (sec.)	CS disc		CS-SG disc	
	Exp. temp. (°C)	FEA temp. (°C)	Exp. temp. (°C)	FEA temp. (°C)
30	128	139.66	125	130.89
60	184	165.68	168	155.11
90	213	191.70	201	179.32
120	240	217.72	227	203.52
150	273	243.73	253	227.70
180	289	269.74	269	251.87
210	314	295.75	285	276.03
240	325	321.76	286	300.18

(a) SL disc

(b) CD disc

(c) CS disc

(d) CS-SG disc

Fig. 5. Heat generation on different kind of brake discs.

3. Results and discussion

3.1 Heat generation

Experimental and FEA results are given in Table 2 for the generation of heat on the disc surfaces. Disc surface temperatures increase with increasing braking time for all disc configurations. However, heat generation is remarkably reduced

(a) SL disc
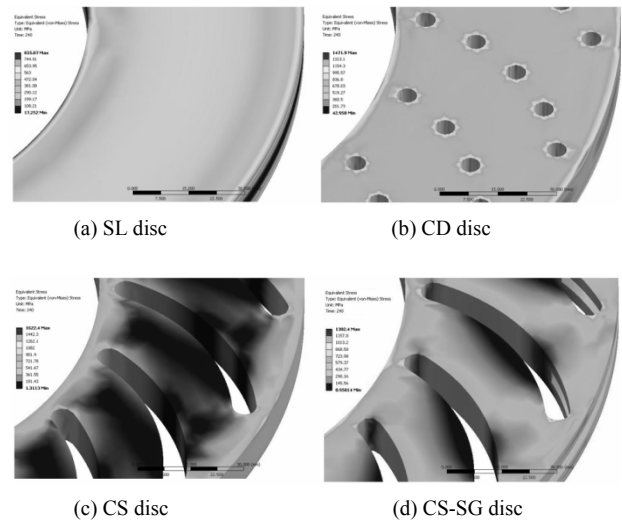
(b) CD disc

(c) CS disc

(d) CS-SG disc

Fig. 6. Thermo-structural behaviors of different kinds of ventilated and solid brake discs.

by ventilation applications. The friction coefficient between brake pad and disc surfaces decreases depending on the temperature rise [19, 20]. Hence, maintaining friction properties of the pads at high temperatures is possible by self-ventilation on the discs under continuous braking conditions.

Fig. 5 shows the temperature distributions on the disc surfaces by FEA at the end of 240 s. The maximum temperature generation occurred in the middle regions of all disc configurations, similar with related studies [12, 14]. However, the temperature region moves from the middle region of the disc to the inner region due to the additional side-cooling in the CS-SG disc configuration. The maximum heat generation on solid disc surfaces is reduced around 4% in the CD disc design. On the other hand, while the maximum heat generation on solid disc surfaces is reduced around 19% in the CS design, it is reduced around 24% in the CS-SG design. Thus, it is beneficial to investigate the thermal stress behavior of these designs.

3.2 Thermal stresses

Fig. 6 shows thermal stress distributions on the disc surfaces by FEA. Ventilation applications increase the thermal stresses on the brake discs. Maximum thermal stress is localized on the corner of the inner and outer edges of the solid disc surfaces. In the case of the CD disc configuration, the maximum stress is located in the inner surfaces of the holes. For the CS and CS-SG disc configurations, maximum stress formations are mainly localized around the slot surfaces close to the inner and outer points of the disc. Hence, the specific regions, where maximum stresses are seen, should be strengthened to prevent potential crack and fatigue problems. One of the possible solutions is the design of different heat dissipation surfaces for ventilated brake discs. Therefore, more homogenous heat convection from the rotor can be provided for the disc surfaces.
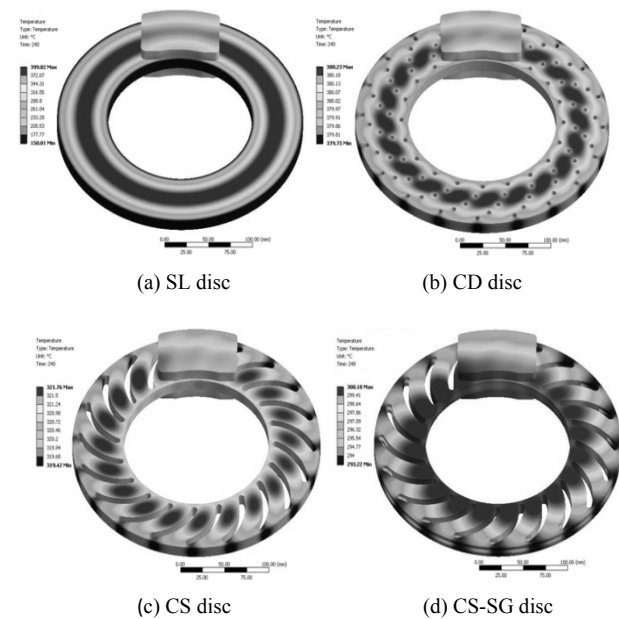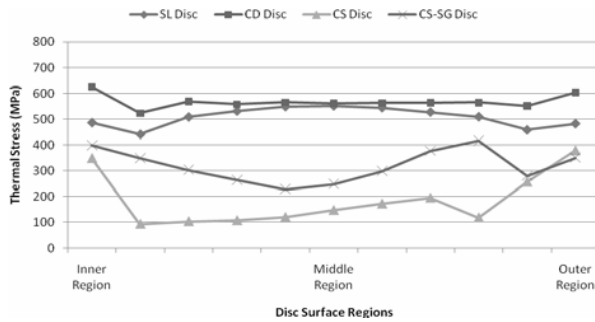
Fig. 7. Thermal stress variations according to disc surface regions.

This is proven by the CS-SG design where the maximum stress generation on the ventilated brake discs is reduced.

In this study, additional thermal stress dissipation on disc surfaces was also investigated. Fig. 7 shows the dissipation characteristics. Heat dissipation surfaces between hole and slot arcs of CD, CS and CS-SG discs were determined to examine stresses where dense friction occurs between the pad and the disc. The maximum stress locations for ventilated brake discs are seen in Fig. 6. The thermal stresses are reduced from the center point between the disc and the pad surfaces toward the inner and outer regions of the disc surfaces for the SL configuration. However, stress distributions on the CD disc surfaces are more homogenous in comparison with the solid disc. For the CS disc configuration, while the stresses are reduced on the frictional surfaces, they gradually increase toward the inner and outer surfaces of the discs, similar with the CS-SG disc configuration. These results will cause a stable wear rate on the pad and disc surfaces of the SL and the CD discs. On the other hand, wear rates will be unstable with the CS and the CS-SG discs.

4. Conclusions

In this study, three different ventilated discs were modeled and their thermo-structural behaviors investigated. The experimental study verified the FEA results for heat generation on the disc surfaces. The following conclusions were drawn:

Heat generation on the solid brake disc surfaces are reduced to a maximum of 24% by ventilation applications. The experimental study verifies the finite element temperature analysis results in the range between 1.13% and 10.87%. This result will positively affect the braking performance by maintaining the friction coefficient between the pad and the disc surface, and by stabilizing the wear rate of the pad surface especially under continuous braking conditions.

Thermal stress formations are higher with ventilated brake discs (CD, CS and CS-SG discs) in comparison to those with solid discs. However, maximum stress formation is reduced to 11% and 19% in an alternative CS-SG disc configuration in comparison to other ventilated disc designs. Thus, CS-SG discs can more effectively reduce heat generation and thermal stresses among ventilated brake discs.

In this study, to increase the heat transfer from the brake discs and to reduce the disc surface temperature on the total surface area of the brake discs, the heat transfer coefficients are gradually increased by employing ventilation applications.

Acknowledgment

Nomenclature————————————————————

A	: Surface area of the rotor
A_f	: Cross-sectional area of front pistons
A_{ins}	: Inlet area of the hole or slot-shaped vanes
A_m	: Cross-sectional area of the master cylinder
A_{out}	: Outlet area of the hole or slot-shaped vanes
D	: Outer diameter of the disc
d	: Inner diameter of the disc
d_h	: Hydraulic diameter
F	: Force on foot pedal
F_f	: Force on each front cylinder piston
h	: Convection heat transfer coefficient
h_R	: Heat transfer coefficient
k_a	: Thermal conductivity of the air
l	: Length of the cooling vane
m_a	: Mass flow rate of air
n_T	: Revolutions per minute
p_n	: Number of pistons
Pr	: Prandtl number
Q	: Rate of heat transfer
Re	: Reynolds number
T_∞	: Ambient air temperature
T_s	: Surface temperature
$V_{average}$	: Average velocity
ρ_a	: Density of air

References

[1] T. C. Chatterley and M. P. Macnaughtan, Cast iron brake discs-current position, performance and future trends in Europe (1999) *SAE* 1999-108-1, 505-514.

[2] G. S. Patrick, An improved rotor for self-ventilating disc brakes, *International Application Published under the Patent Cooperation Treaty (PCT)* (2002) WO/2002/064992.

[3] M. D. Hudson and R. L. Ruhl, Ventilated brake rotor air flow investigation, *SAE*, 971033 (1997).

[4] B. Breuer and K. H. Bill, *Brake technology handbook*, First English Edition, SAE International, Warrandale, Pennsylvania, USA (2008).

[5] R. Limpert, *Brake design and safety*, Second Edition, Society of Automotive Engineers, Inc. Warrendale USA (1999) 140-143.

[6] Ch. Zuber and B. Heidenreich, Development of a net shape

manufacturing mehod for ventilated brake discs in single piece design, *Materialwissenschaft und Werkstofftechnik*, 37 (4) (2006) 301-308.

[7] D. B. Antanaitis and A. Rifici, The effect of rotor crossdrilling on brake performance (2006) *SAE*, 2006-01-0691, 571-596.

[8] D. Aleksendric, C. Duboka, P. F. Gotowicki, G. V. Mariotti and V. Nigrelli, Braking procedure analysis of a pegs-wing ventilated disk brake rotor, *International Journal of Vehicle System Modelling and Testing* (2006) 1, 4, 233-252.

[9] G. Venkitachalam and M. Maharudrappa, Flow and heat transfer analysis of a ventilated disc brake rotor using CFD, *SAE*, 2008-01-0822 (2008).

[10] S. B. Park, K. S. Lee and D. H. Lee, An investigation of local heat transfer characteristics in a ventilated disc brake with helically fluted surface, *Journal of Mechanical Science and Technology,* 21 (2007) 2178-2187.

[11] Y. Yildiz and M. Duzgun, Stress analysis of ventilated brake discs with finite element method, International *Journal of Automotive Technology,* 11 (1) (2010) 133-138.

[12] D. J. Kim, Y. M. Lee, J. S. Park and C. S. Seok, Thermal stress analysis for a disk brake of railway vehicles with consideration of the pressure distribution on a frictional surface, *Materials Science and Engineering A* (2008) 483-484, 456-459.

[13] F. Bagnoli, F. Dolce and M. Bernabei, Thermal fatigue cracks of fire fighting vehicles gray iron brake discs, *Engineering Failure Analysis,* 16 (1) (2009) 152-163.

[14] P. Hwang and X. Wu, Investigation of temperature and thermal stress in ventilated disc brake based on 3D thermo-mechanical coupling model, *Journal of Mechanical Science and Technology,* 24 (2010) 81-84.

[15] T. J. Mackin et al., Thermal cracking in disc breaks, *Engineering Failure Analysis*, 9 (2002) 63-76.

[16] T. K. Kao, J. W. Richmond and A. Douarre, Brake disc hot spotting and thermal judder: an experimental and finite element study, *International Journal of Vehicle Design*, 23 (3/4) (2000) 276-296.

[17] J. N. Han, N. J. Cho, S. W. Chae and Y. Choi, Hybrid three-dimensional mesh generation from quad-dominant surface meshes, *International Journal of Automotive Technology*, 9 (5) (2008) 633-640.

[18] H. Heisler, *Vehicle and engine technology*, Second Edition, SAE, 400 Commonwealth Drive, Warrendale, PA 15096-0001, U.S.A (1999).

[19] R. Sturm, Brakes and ABS on four wheel drive vehicles, *SAE* (1988) 880321.

[20] A. Vries and M. Wagner, The brake judder phenomenon, *SAE* (1992) 920554.

Mesut Duzgun, Ph.D is an Assistant Professor in the Automotive Engineering Department, Faculty of Technology at Gazi University (2001-present). He received his MSc and Ph.D from the Institute of Science and Technology at Gazi University in Turkey. He has 16 years of experience in the automotive industry and the academia. His current research interests are in the areas of automotive engineering, vehicle dynamics, vehicle tests and test equipment, brake system, Anti-lock Brake System (ABS) Technology, test methodology, vehicle suspension systems, vehicle safety systems, and so on.